Shaping the Biphoton Temporal Waveform with Spatial Light Modulation

Luwei Zhao, Xianxin Guo, Yuan Sun, Yumian Su, M. M. T. Loy, and Shengwang Du*
Department of Physics, The Hong Kong University of Science and Technology, Clear Water Bay, Kowloon, Hong Kong, China
(Received 4 March 2015; published 3 November 2015)

We demonstrate a technique for shaping the temporal wave function of biphotons generated from spatially modulated spontaneous four-wave mixing in cold atoms. We show that the spatial profile of the pump field can be mapped onto the biphoton temporal wave function in the group delay regime. The spatial profile of the pump laser beam is shaped by using a spatial light modulator. This spatial-to-temporal mapping enables the generation of narrow-band biphotons with controllable temporal waveforms.

DOI: 10.1103/PhysRevLett.115.193601 PACS numbers: 42.50.Dv, 42.50.Gy, 42.65.Lm

Generating entangled photon pairs (biphotons) with controllable time-frequency quantum states is of great interest not only for understanding and probing fundamental quantum physics, but also for developing advanced technologies in quantum information processing. For wideband (> THz) biphotons produced from spontaneous parametric down-conversion (SPDC), the two-photon state can be engineered by coherently manipulating its joint spectrum after the biphoton generation [1–3]. Modulating the phase matching condition inside the nonlinear crystal, mapping of the spatial feature of the pump beam into the biphoton joint spectrum has been demonstrated [4]. Making use of a spatially chirped quasi-phase-matching crystal, it is possible to produce single-cycle biphotons [5,6]. However, these methods do not work for narrow-band (MHz) biphotons. Recent protocols of memory-based quantum networks [7–10] require narrow-band photon pairs [11–17] that can interact with atoms efficiently. Storing and coupling these narrow-band single photons into atoms and cavities efficiently require they have optimal temporal waveforms [18–22]. Using an external electro-optic modulator (EOM), narrow-band biphotons can be employed to obtain heralded single photons with arbitrarily shaped temporal waveforms [23], but this introduces unavoidable waveform-shaping loss and reduces the heralding efficiency [19–21]. For narrow-band biphotons generated from spontaneous four-wave mixing (SFWM) [24], modulating both driving lasers can transfer the classical field correlation onto the biphoton waveform [25,26], but this temporal waveform shaping reduces the frequency entanglement because of the breakdown of the time translation symmetry.

In this Letter, we demonstrate a new technique of shaping the biphoton temporal wave function in the narrow-band SFWM process, by directly mapping the spatial profile of the pump laser beam onto the biphoton temporal waveform. The related atomic level diagram is shown in Fig. 1(a), where the atoms are prepared in the ground state $|1\rangle$. In the presence of a pump (ω_p, E_p) and coupling (ω_c, E_c) laser fields, Stokes (ω_S) and anti-Stokes (ω_{aS}) photon pairs are spontaneously generated. The pump laser is far-detuned by Δ_p from the transition $|1\rangle \rightarrow |4\rangle$, and the coupling laser is on resonance to the transition $|2\rangle \rightarrow |3\rangle$. While the Stokes photon moves nearly at the speed of light in vacuum (c), the anti-Stokes photon travels with a slow group velocity V_g because of the electromagnetically induced transparency (EIT) [27]. An ideal schematic of realizing SFWM spatial-to-temporal mapping is illustrated in Fig. 1(b), where the pump and coupling laser beams are counterpropagating. The wavelengths of the two driving lasers are chosen such that the phase-matched photon pairs can be produced at a right angle in the opposite directions along the z axis. The coupling field dresses the atomic medium uniformly. The pump beam passes through a mask whose profile $f_p(z)$ is projected onto the atomic cloud. As a result, the photon-pair generation probability amplitude is spatially modulated following $\chi^{(3)} E_c E_p f_p(z) \hat{a}^\dagger_{aS} \hat{a}^\dagger_S$, where $\chi^{(3)}$ is the 3rd-order nonlinear susceptibility. $\hat{a}^\dagger_S$ and $\hat{a}^\dagger_{aS}$ are the Stokes and anti-Stokes field creation operators. Because the anti-Stokes photon travels slowly at V_g, it experiences a different time delay if generated at a different position. Therefore, at the two detectors (D_S and D_{aS}) located outside the medium, we have a linear mapping between the registered two-photon relative arrival time delay $\tau = t_{aS} - t_s$ and the generation position z inside the medium: $\tau \Leftrightarrow z$. As a result, the photon pair generation spatial amplitude [$\propto f_p(z)$] is mapped to the two-photon joint detection probability amplitude $\psi(\tau)$. We thus code the spatial information of the pump spatial profile to the sequential temporal waveform of the biphoton quantum state.

Although the above conceptual picture is clear and straightforward, to our best knowledge, such a spatial-to-temporal mapping in biphoton generation has never been experimentally demonstrated. For SPDC wideband (>THz) biphotons, it is impossible to directly resolve this effect by the temporal resolution of single photon counters.

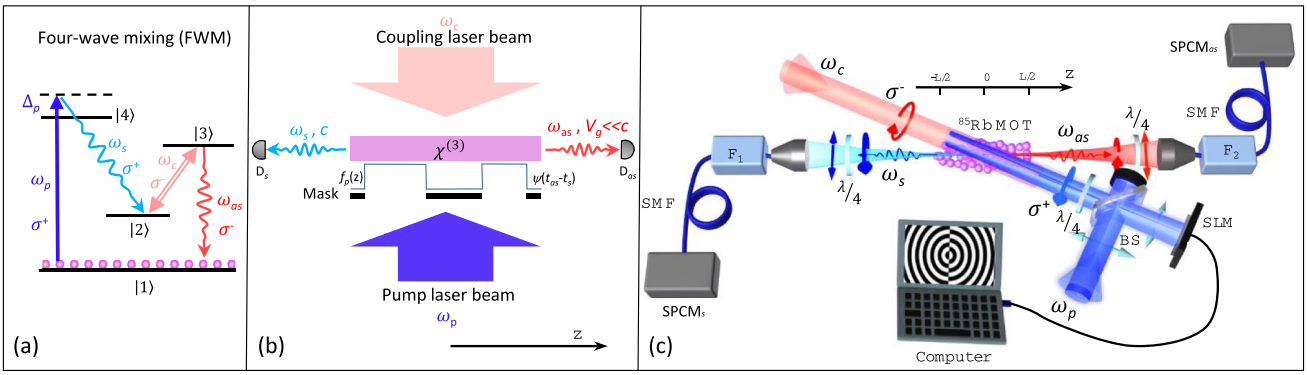

FIG. 1 (color online). SFWM biphoton generation with spatial-to-temporal mapping. (a) ^{85}Rb atomic energy level diagram: $|1\rangle = |5S_{1/2}, F = 2\rangle$, $|2\rangle = |5S_{1/2}, F = 3\rangle$, $|3\rangle = |5P_{1/2}, F = 3\rangle$, and $|4\rangle = |5P_{3/2}, F = 3\rangle$. (b) An ideal spatial-to-temporal mapping model with right-angle geometry for illustration purpose. (c) Experimental setup. $\lambda/4$: quarter-wave plate, ↕: linear polarizer, F_1 and F_2: frequency filters with 0.5 GHz bandwidth, SMF: single-mode fiber, SPCM: single-photon counting module, BS: beam splitter, and SLM: spatial light modulator.

The model picture of Fig. 1(b) is based on the EIT-assisted SFWM where Stokes and anti-Stokes photons travel with different group velocities. To allow at least two temporal modes produced and traveling through the medium, the EIT needs a sufficient delay-bandwidth product that requires the atomic optical depth (OD) on the anti-Stokes transition meet OD > 62 [28]. However, at such a high OD, the EIT loss becomes significant at the right-angle geometry because of the Doppler-effect-induced ground-state decoherence and other dephasing mechanisms. In this Letter, we show that, although the right-angle geometry is easy to understand, it is not necessary. We use a phase spatial light modulator (SLM) to shape the pump beam and project its spatial field profile onto the atomic medium at a small angle that holds the EIT at a high OD.

Figure 1(c) illustrates our experimental setup. We work with ^{85}Rb cold atoms in a dark-line two-dimensional magneto-optical trap (MOT) [30], with a length $L = 1.5$ cm along its longitudinal z axis. The experiment is run periodically: in each cycle, a 4.5-ms trapping time window is followed by a 0.5-ms biphoton generation. A weak linearly polarized pump (780 nm, $\Delta_p = 2\pi \times 110$ MHz) laser beam with a collimated beam diameter of 2.2 mm is retroreflected by a phase SLM (Holoeye, LETO). Then it becomes σ^+ circularly polarized after passing through a quarter-wave plate and is incident to the atoms with an angle of 2.2° to the z axis. A coupling (σ^-, 795 nm) laser beam, with a collimated beam diameter of 1.4 mm, counterpropagates with respect to the pump beam. The Stokes (σ^+, 780 nm) and anti-Stokes (σ^-, 795 nm) photons are collected by two single-mode fibers (SMFs) along the z axis with a 250-μm-waist Gaussian mode focused on the MOT center, and then detected by two single-photon counting modules (SPCM$_S$ and SPCM$_{aS}$, PerkinElmer, SPCM-AQ4C). The quarter-wave plates and polarizers on each side before fiber coupling act as polarization filters. The two-photon coincidence counts are analyzed with a bin width $\Delta t_{\text{bin}} = 2$ ns.

The spatial profile of the pump beam is controlled by the phase SLM. As shown in Fig. 1(c), the z axis is defined along the anti-Stokes photon propagation direction, which has a small angle of 2.2° to the pump beam direction. As a result, the pump beam transverse directions are not perpendicular to the z axis and its transverse profile is therefore projected to the z axis. The pump Rabi frequency spatial distribution along the z axis can be characterized as $\Omega_p(z) = \Omega_{p0} f_p(z)$, where $f_p(z)$ satisfies $\int_{-L/2}^{L/2} |f_p(z)|^2 dz = L$. In this work, we also carefully take into account the slowly varying envelope of the pump beam along its propagation direction. To fulfill the delay-bandwidth condition, we work at OD $= 120$. Other fixed parameters are $\Omega_{p0} = 2\pi \times 1.0$ MHz and $\Omega_c = 2\pi \times 11.0$ MHz. Under these conditions, the EIT group delay is about $\tau_g = L/V_g = 924$ ns. In the group delay regime, we obtain the biphoton relative temporal wave function approximately as

$$\psi(\tau) \simeq \kappa_0 V_g f_p(L/2 - V_g \tau), \tag{1}$$

where κ_0 is the nonlinear coupling coefficient. The detailed derivation is provided in Ref. [31]. As shown in Eq. (1), the projected pump field spatial profile $f_p(z)$ is transferred onto the biphoton temporal wave function with a scaling factor of V_g.

We first characterize the biphoton source without using the SLM. In this case, the pump beam transverse Gaussian profile is projected to the biphoton propagation z axis, shown as a slowly varying Gaussian envelop in Fig. 2(a1). The biphoton temporal correlation, measured as coincidence counts over $T = 3000$ s, is plotted in Fig. 2(a2). With a joint-detection efficiency $\beta = 5\%$ and duty cycle $\zeta = 10\%$, the coincidence counts can be calculated from

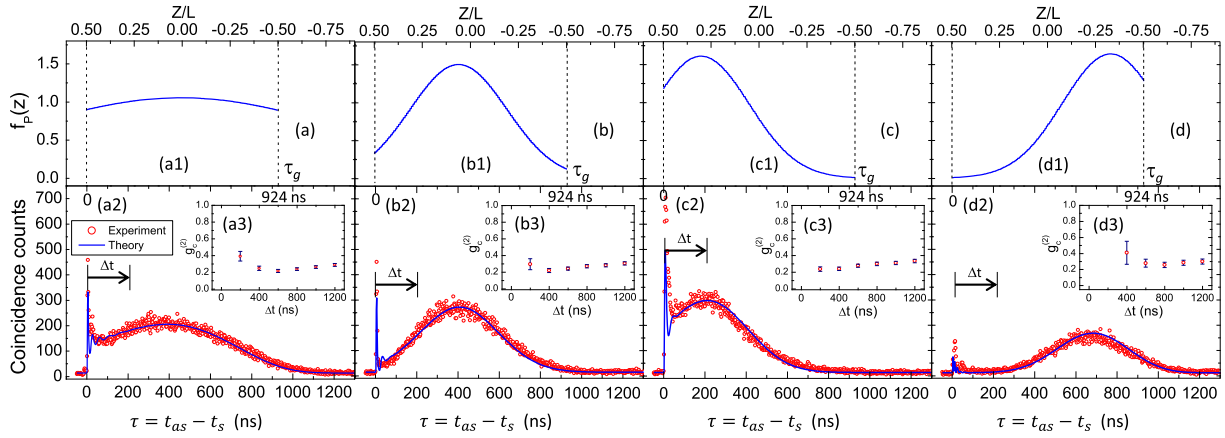

FIG. 2 (color online). Biphoton waveforms with Gaussian shapes. (a) The wide Gaussian shape is produced from the collimated pump beam. (b) The narrow Gaussian shape is produced by focusing the pump beam to the center of the MOT. In (c) and (d), the Gaussian shapes are shifted by moving the pump beam focus spot to the two ends of the MOT. [(a1), (b1), (c1), and (d1)]: the pump beam profile along z axis, [(a2), (b2), (c2), and (d2)]: the corresponding coincidence counts collected for 3000 s, [(a3), (b3), (c3), and (d3)]: the measured $g_c^{(2)}$ of heralded single anti-Stokes photons.

$C(\tau) = \beta\zeta|\psi(\tau)|^2\Delta t_{\mathrm{bin}}T$. The correlation time of about 1 μs agrees well with our group delay picture. The spike-like oscillatory structure at the leading edge is the optical precursor, which cannot be slowed down by the EIT effect [32]. We then focus the pump beam tightly, close to the MOT center with a waist diameter of 0.46 mm and plot its profile projection on the z axis in Fig. 2(b1). The resulting Gaussian-shaped biphoton waveform is shown in Fig. 2(b2). By moving the focus spot along the z axis, we observe that the Gaussian profile shifts in the biphoton waveform accordingly in Figs. 2(c) and 2(d), as predicted by Eq. (1). The solid curves in Figs. 2(a2)–2(d2), calculated from the theory described in Ref. [31], agree well with the experiment.

We confirm the nonclassical property of the biphoton source by verifying its violation of the Cauchy-Schwarz inequality [33]. Normalizing the coincidence counts to the accidental background, we obtain the normalized cross-correlation $g^{(2)}_{\mathrm{S,aS}}(\tau)$ with peak values of 33.9, 32.4, 52.5, and 16.1 for Figs. 2(a2)–2(d2), respectively. With the measured autocorrelations $g^{(2)}_{\mathrm{S,S}}(0) = 1.92$ and $g^{(2)}_{\mathrm{aS,aS}}(0) = 1.88$, we verify that the Cauchy-Schwarz inequality $[g^{(2)}_{\mathrm{S,aS}}(\tau)]^2/[g^{(2)}_{\mathrm{S,S}}(0)g^{(2)}_{\mathrm{aS,aS}}(0)] \leq 1$ is violated by factors of 318, 290, 764, and 72, for the data in Figs. 2(a2)–2(d2), respectively. We further confirm the quantum nature of the photon source by measuring the conditional autocerrelation function $g_c^{(2)}$ of the heralded single anti-Stokes photons [34]. The measured $g_c^{(2)}$ as a function of coincidence window width are displayed in Figs. 2(a3)–2(d3). In all these cases, $g_c^{(2)} < 0.5$ holds well within the entire temporal waveform and indicates the near single-photon character [35].

Single photons with exponential waveforms are desirable for many applications, such as efficient absorption by two-level atoms [20] and coupling to an optical cavity [21,22]. Here we show that controllable exponential biphoton waveforms can be obtained by shaping the pump beam spatial profile. We use the SLM to modulate the pump beam and obtain its field profiles along the z axis shown in Fig. 3(a). The resulting biphoton waveforms in Fig. 3(b) decay nearly exponentially (fitted with $e^{-\gamma\tau}$) with time constants of 119 and 206 ns. For these two cases, both

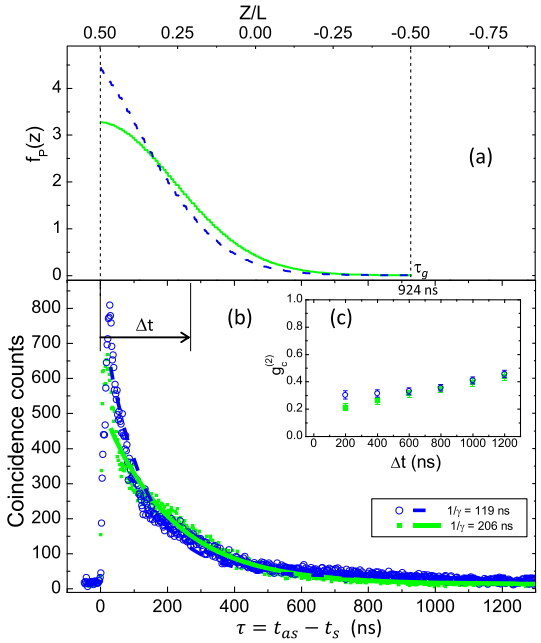

FIG. 3 (color online). Biphoton exponential waveforms with different time constants. (a) Pump beam profiles along z axis. (b) Two-photon coincidence counts as functions of relative time delay. (c) The measured $g_c^{(2)}$ of heralded single anti-Stokes photons.

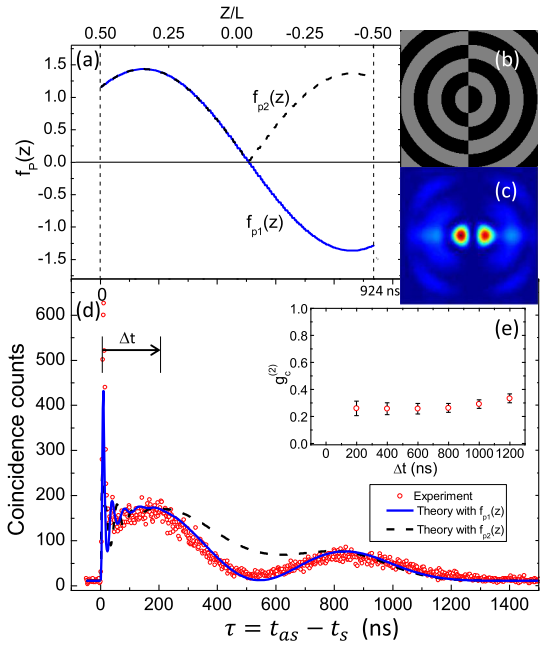

FIG. 4 (color online). Biphoton waveform with a double-peak structure. (a) The pump field spatial profile projected onto the z axis. (b) The phase pattern input to the SLM. (c) The transverse intensity distribution of the pump beam. (d) The coincidence counts collected over 3000 s. (e) The measured $g_c^{(2)}$ of heralded single anti-Stokes photons.

violate the Cauchy-Schwarz inequality by factors of 707 and 510. The measured $g_c^{(2)}$ of the heralded anti-Stokes photons is plotted in Fig. 3(c). From these biphotons, we can generate heralded anti-Stokes photons with an exponential-decay waveform triggered by the Stokes photons, or heralded Stokes photons with an exponential-growth waveform triggered by the anti-Stokes photons following a time-reverse process [21,36]. We can also use a single-sided cavity to convert an exponential decay waveform to an exponential growth waveform [22].

We further demonstrate the ability to shape the biphoton waveform into two separated temporal modes. The pump field spatial profile $f_{p1}(z)$ is plotted as the solid curve in Fig. 4(a), with an amplitude node near the MOT center and a π phase jump across $z = 0$. This field spatial profile is created by inputting the phase pattern shown in Fig. 4(b) to the SLM. The pump intensity transverse distribution is displayed in Fig. 4(c). This pump spatial modulation leads to a biphoton temporal correlation with double peaks shown in Fig. 4(d). The spatial phase variation of the pump beam is also mapped onto the biphoton waveform. This can be indirectly proved by the perfect agreement between the theory (solid curve) and experiment (circular points) in Fig. 4(d). To further clarify this, we maintain the pump intensity spatial profile but change the filed profile function to $f_{p2}(z) = |f_{p1}(z)|$, the corresponding theoretical waveform is shown as the dashed curve in Fig. 4(d), which deviates a lot from the experimental data. Therefore, the pump field spatial modulation shapes the complex temporal wave function (amplitude + phase) of the biphotons. If the background accidental coincidence counts are removed, we obtain a visibility of 88.4% for the waveform modulation. This near-unity visibility also suggests the phase distribution of the biphoton temporal wave function $\psi(\tau)$ follows the pump field profile $f_p(L/2 - V_g\tau)$, though the measurement of the coincidence counts only reveals $|\psi(\tau)|^2$. For this case, the Cauchy-Schwarz inequality is violated by a factor of 881. The measured $g_c^{(2)}$ of heralded anti-Stokes photons [Fig. 4(e)] confirms the quantum nature of the source.

In summary, we demonstrate shaping the biphoton temporal wave function by spatially modulating the pump laser field profile. Using a SLM, we produce biphotons with temporal waveforms of Gaussian, exponential, and double-peak shapes. Taking into account the SMF fiber-fiber coupling efficiency (70%), filter transmission (54% each), SPCM efficiency (50% each), and duty cycle (10%), we estimate the photon pair generation rate to be about 4000 pairs/s. A higher biphoton rate can be achieved by increasing the pump power. Our proof-of-principle demonstration can be extended to generate narrow-band biphotons with arbitrarily shaped waveforms. This can be achieved by calculating the required pump beam spatial profile and then the phase pattern of the SLM. Or alternatively, one can use the measured biphoton coincidence as a feedback to adjust the phase pattern of SLM until the desired waveform is obtained. This spatial-to-temporal biphoton shaping can be used to produce heralded narrow-band single photons with controllable waveforms. We measure the heralding efficiency of generating a single anti-Stokes photon, under the condition of detecting a Stokes photon. The heralding efficiency for the case with a collimated pump beam [Fig. 2(a)] is 92%. With the SLM, the heralding efficiencies become 88%, 90%, 70%, and 74%, for the cases in Figs. 2(b), 2(c), 2(d), and Fig. 4, respectively. Therefore, it is nearly lossless in generating heralded single photons as compared to the external EOM method in Ref. [23]. It can be immediately applied to improve the photon-cavity loading efficiency in a quantum network [21].

The work was supported by the Hong Kong Research Grants Council (Project No. 601113).

*Corresponding author.
dusw@ust.hk

[1] A. Peer, B. Dayan, A. A. Friesem, and Y. Silberberg, Temporal Shaping of Entangled Photons, Phys. Rev. Lett. **94**, 073601 (2005).

[2] M. Hendrych, X. Shi, A. Valencia, and J. P. Torres, Broadening the bandwidth of entangled photons: A step towards the generation of extremely short photons, Phys. Rev. A **79**, 023817 (2009).

[3] C. Bernhard, B. Bessire, T. Feurer, and A. Stefanov, Shaping frequency-entangled qudits, Phys. Rev. A **88**, 032322 (2013).
[4] A. Valencia, A. Cere, X. Shi, G. Molina-Terriza, and J. P. Torresx, Shaping the Waveform of Entangled Photons, Phys. Rev. Lett. **99**, 243601 (2007).
[5] S. E. Harris, Chirp and Compress: Toward Single-Cycle Biphotons, Phys. Rev. Lett. **98**, 063602 (2007).
[6] S. Sensarn, G. Y. Yin, and S. E. Harris, Generation and Compression of Chirped Biphotons, Phys. Rev. Lett. **104**, 253602 (2010).
[7] L.-M. Duan, M. D. Lukin, J. I. Cirac, and P. Zoller, Long-distance quantum communication with atomic ensembles and linear optics, Nature (London) **414**, 413 (2001).
[8] B. Zhao, Z.-B. Chen, Y.-A. Chen, J. Schmiedmayer, and J.-W. Pan, Robust Creation of Entanglement between Remote Memory Qubits, Phys. Rev. Lett. **98**, 240502 (2007).
[9] A. Kuzmich, W. P. Bowen, A. D. Boozer, A. Boca, C. W. Chou, L.-M. Duan, and H. J. Kimble, Generation of nonclassical photon pairs for scalable quantum communication with atomic ensembles, Nature (London) **423**, 731 (2003).
[10] H. J. Kimble, The quantum internet, Nature (London) **453**, 1023 (2008).
[11] V. Balic, D. A. Braje, P. Kolchin, G. Y. Yin, and S. E. Harris, Generation of Paired Photons with Controllable Waveforms, Phys. Rev. Lett. **94**, 183601 (2005).
[12] X.-H. Bao, Y. Qian, J. Yang, H. Zhang, Z.-B. Chen, T. Yang, and J.-W. Pan, Generation of Narrow-Band Polarization-Entangled Photon Pairs for Atomic Quantum Memories, Phys. Rev. Lett. **101**, 190501 (2008).
[13] S. Du, P. Kolchin, C. Belthangady, G. Y. Yin, and S. E. Harris, Subnatural Linewidth Biphotons with Controllable Temporal Length, Phys. Rev. Lett. **100**, 183603 (2008).
[14] L. Zhao, X. Guo, C. Liu, Y. Sun, M. M. T. Loy, and S. Du, Photon pairs with coherence time exceeding 1 μs, Optica **1**, 84 (2014).
[15] K. Liao, H. Yan, J. He, S. Du, Z.-M. Zhang, and S.-L. Zhu, Subnatural-Linewidth Polarization-Entangled Photon Pairs with Controllable Temporal Length, Phys. Rev. Lett. **112**, 243602 (2014).
[16] Y.-W. Cho, K.-K. Park, J.-C. Lee, and Y.-H. Kim, Engineering Frequency-Time Quantum Correlation of Narrow-Band Biphotons from Cold Atoms, Phys. Rev. Lett. **113**, 063602 (2014).
[17] D.-S. Ding, W. Zhang, Z.-Y. Zhou, S. Shi, G.-Y. Xiang, X.-S. Wang, Y.-K. Jiang, B.-S. Shi, and G.-C. Guo, Quantum Storage of Orbital Angular Momentum Entanglement in an Atomic Ensemble, Phys. Rev. Lett. **114**, 050502 (2015).
[18] S. Zhang, J. F. Chen, C. Liu, M. M. T. Loy, G. K. L. Wong, and S. Du, Optical Precursor of a Single Photon, Phys. Rev. Lett. **106**, 243602 (2011).
[19] S. Zhou, S. Zhang, C. Liu, J. F. Chen, J. Wen, M. M. T. Loy, G. K. L. Wong, and S. Du, Optimal storage and retrieval of single-photon waveforms, Opt. Express **20**, 24124 (2012).
[20] S. Zhang, C. Liu, S. Zhou, C.-S. Chuu, M. M. T. Loy, and S. Du, Coherent Control of Single-Photon Absorption and Reemission in a Two-Level Atomic Ensemble, Phys. Rev. Lett. **109**, 263601 (2012).
[21] C. Liu, Y. Sun, L. Zhao, S. Zhang, M. M. T. Loy, and S. Du, Efficiently Loading a Single Photon into a Single-Sided Fabry-Perot Cavity, Phys. Rev. Lett. **113**, 133601 (2014).
[22] B. Srivathsan, G. K. Gulati, A. Cere, B. Chng, and C. Kurtsiefer, Reversing the Temporal Envelope of a Heralded Single Photon using a Cavity, Phys. Rev. Lett. **113**, 163601 (2014).
[23] P. Kolchin, C. Belthangady, S. Du, G. Y. Yin, and S. E. Harris, Electro-Optic Modulation of Single Photons, Phys. Rev. Lett. **101**, 103601 (2008).
[24] S. Du, J. Wen, and M. H. Rubin, Narrowband biphoton generation near atomic resonance, J. Opt. Soc. Am. B **25**, C98 (2008).
[25] S. Du, J. Wen, and C. Belthangady, Temporally shaping biphoton wave packets with periodically modulated driving fields, Phys. Rev. A **79**, 043811 (2009).
[26] J. F. Chen, S. Zhang, H. Yan, M. M. T. Loy, G. K. L. Wong, and S. Du, Shaping Biphoton Temporal Waveforms with Modulated Classical Fields, Phys. Rev. Lett. **104**, 183604 (2010).
[27] S. E. Harris, Electromagnetically induced transparency, Phys. Today **50**, 36 (1997).
[28] See the Supplemental Material http://link.aps.org/supplemental/10.1103/PhysRevLett.115.193601, which includes Ref. [29], for the derivation of the delay-bandwidth condition and the biphoton waveforms at a low OD of 30.
[29] S. E. Harris and L. V. Hau, Nonlinear Optics at Low Light Levels, Phys. Rev. Lett. **82**, 4611 (1999).
[30] S. Zhang, J. F. Chen, C. Liu, S. Zhou, M. M. T. Loy, G. K. L. Wong, and S. Du, A dark-line two-dimensional magneto-optical trap of ^{85}Rb atoms with high optical depth, Rev. Sci. Instrum. **83**, 073102 (2012).
[31] L. Zhao, Y. Su, and S. Du, Narrowband Biphoton Generation in the Group Delay Regime, arXiv:1409.3341.
[32] S. Zhang, J. F. Chen, C. Liu, M. M. T. Loy, G. K. L. Wong, and S. Du, Optical Precursor of a Single Photon, Phys. Rev. Lett. **106**, 243602 (2011).
[33] M. D. Reid and D. F. Walls, Violations of classical inequalities in quantum optics, Phys. Rev. A **34**, 1260 (1986).
[34] P. Grangier, G. Roger, and A. Aspect, Experimental evidence for a photon anticorrelation effect on a beam splitter: A new light on single-photon interferences, Europhys. Lett. **1**, 173 (1986).
[35] A classical source gives $g_c^{(2)} \geq 1$ and shows the bunching effect. A two-photon Fock state gives $g_c^{(2)} \geq 0.5$. A pure single-photon state gives $g_c^{(2)} \geq 0$ because a single photon on the beam splitter can only go to one output port or the other.
[36] G. K. Gulati, B. Srivathsan, B. Chng, A. Cere, D. Matsukevich, and C. Kurtsiefer, Generation of an exponentially rising single-photon field from parametric conversion in atoms, Phys. Rev. A **90**, 033819 (2014).